

Smart Race cDNA amplification kit (Clontech). Expressed sequence tags were amplified by PCR with the universal adapter primer provided with the kit and the various, specific internal primers.

Complete macronuclear gene-sized chromosomes

Telomere-specific primers in combination with internal gene sequences allow a straightforward recovery of the complete gene³⁰. The specific (internal) primers were based on the DNA sequences of internal fragments of the various genes, which were recovered previously by PCR with degenerated primers for conserved parts of the various genes.

Phylogenetic analysis

Protein sequences were aligned with ClustalW and Muscle; unequivocally aligned positions were selected with Gblocks or manually. Phylogenies were inferred with maximum likelihood by using a discrete gamma-distribution model with four rate categories plus invariant positions and the Poisson amino acid similarity matrix, and neighbour joining as implemented in ClustalW, correcting for multiple substitutions with the Gonnert amino acids identity matrix, and bootstrapping with 100 samples.

ORFs with a lower size limit of 100 nucleotides were identified with ORF Finder (<http://www.ncbi.nlm.nih.gov/gorf/gorf.html>). tRNAs were identified with tRNAscan-SE (<http://www.genetics.wustl.edu/eddy/tRNAscan-SE>). Potential mitochondrial import signals were detected with MITOP (<http://mips.gsf.de/cgi-bin/proj/medgen/mitofilter>). Sequence searches were performed with BLASTX (<http://www.ncbi.nlm.nih.gov/BLAST>), BLASTN and FASTA. For references on phylogenetic analysis see Supplementary Information.

Received 18 August 2004; accepted 7 January 2005; doi:10.1038/nature03343.

1. Müller, M. The hydrogenosome. *J. Gen. Microbiol.* **39**, 2879–2889 (1993).
2. Roger, A. J. Reconstructing early events in eukaryotic evolution. *Am. Nat.* **154**, S146–S163 (1999).
3. Tielens, A. G. M., Rotte, C., van Hellemond, J. J. & Martin, W. Mitochondria as we don't know them. *Trends Biochem. Sci.* **27**, 564–572 (2002).
4. Embley, T. M. *et al.* Hydrogenosomes, mitochondria and early eukaryotic evolution. *IUBMB Life* **55**, 387–395 (2003).
5. Dyall, S. D., Brown, M. T. & Johnson, P. J. Ancient invasions: From endosymbionts to organelles. *Science* **304**, 253–257 (2004).
6. van der Giezen, M., Sjölloma, K. A., Artz, R. R., Alkema, W. & Prins, R. A. Hydrogenosomes in the anaerobic fungus *Neocallimastix frontalis* have a double membrane but lack an associated organelle genome. *FEBS Lett.* **408**, 147–150 (1997).
7. Clemens, D. L. & Johnson, P. J. Failure to detect DNA in hydrogenosomes of *Trichomonas vaginalis* by nick translation and immunomicroscopy. *Mol. Biochem. Parasitol.* **106**, 307–313 (2000).
8. Leon-Avila, G. & Tovar, J. Mitosomes of *Entamoeba histolytica* are abundant mitochondrion-related remnant organelles that lack a detectable organelle genome. *Microbiol.* **150**, 1245–1250 (2004).
9. Fenchel, T. & Finlay, B. J. *Ecology and Evolution in Anoxic Worlds* (Oxford University Press, Oxford, UK, 1995).
10. Embley, T. M., Horner, D. A. & Hirt, R. P. Anaerobic eukaryote evolution: hydrogenosomes as biochemically modified mitochondria? *Trends Ecol. Evol.* **12**, 437–441 (1997).
11. Voncken, F. *et al.* Multiple origins of hydrogenosomes: functional and phylogenetic evidence from the ADP/ATP carrier of the anaerobic chytrid *Neocallimastix* sp. *Mol. Microbiol.* **44**, 1441–1454 (2002).
12. van der Giezen, M. *et al.* Conserved properties of hydrogenosomal and mitochondrial ADP/ATP carriers: a common origin for both organelles. *EMBO J.* **21**, 572–579 (2002).
13. Martin, W., Hoffmeister, M., Rotte, C. & Henze, K. An overview of endosymbiotic models for the origins of eukaryotes, their ATP-producing organelles (mitochondria and hydrogenosomes), and their heterotrophic lifestyle. *Biol. Chem.* **382**, 1521–1539 (2001).
14. Martin, W. & Müller, M. The hydrogen hypothesis for the first eukaryote. *Nature* **392**, 37–41 (1998).
15. Akhmanova, A. *et al.* A hydrogenosome with a genome. *Nature* **396**, 527–528 (1998).
16. Brunk, C. F., Lee, L. C., Tran, A. B. & Li, J. Complete sequence of the mitochondrial genome of *Tetrahymena thermophila* and comparative methods for identifying highly divergent genes. *Nucleic Acids Res.* **31**, 1673–1682 (2003).
17. Burger, G., Gray, M. W. & Lang, B. F. Mitochondrial genomes: anything goes. *Trends Genet.* **19**, 709–716 (2003).
18. Dyall, S. D. *et al.* Non-mitochondrial complex I proteins in a hydrogenosomal oxidoreductase complex. *Nature* **431**, 1103–1107 (2004).
19. Hrdy, I. *et al.* *Trichomonas* hydrogenosomes contain the NADH dehydrogenase module of mitochondrial complex I. *Nature* **432**, 618–622 (2004).
20. van Hoek, A. H. A. M. *et al.* Multiple acquisition of methanogenic archaeal symbionts by anaerobic ciliates. *Mol. Biol. Evol.* **17**, 251–258 (2000).
21. Degli Esposti, M. Inhibitors of NADH-ubiquinone reductase: an overview. *Biochim. Biophys. Acta* **1364**, 222–235 (1998).
22. Akhmanova, A. *et al.* A hydrogenosome with pyruvate formate-lyase: anaerobic chytrid fungi use an alternative route for pyruvate catabolism. *Mol. Microbiol.* **32**, 1103–1114 (1999).
23. Boxma, B. *et al.* The anaerobic chytridiomycete fungus *Piromyces* sp. E2 produces ethanol via pyruvate:formate lyase and an alcohol dehydrogenase E. *Mol. Microbiol.* **51**, 1389–1399 (2004).
24. van Hellemond, J. J., Klockiewicz, M., Gaasenbeek, C. P. H., Roos, M. H. & Tielens, A. G. M. Rhodoquinone and complex II of the electron transport chain in anaerobically functioning eukaryotes. *J. Biol. Chem.* **270**, 31065–31070 (1995).
25. Sickmann, A. *et al.* The proteome of *Saccharomyces cerevisiae* mitochondria. *Proc. Natl Acad. Sci. USA* **100**, 13207–13212 (2003).
26. Cotter, D., Guda, P., Fahy, E. & Subramaniam, S. MitoProteome: mitochondrial protein sequence database and annotation system. *Nucleic Acids Res.* **32**, D463–D467 (2004).
27. Voncken, F. G. J. *et al.* A hydrogenosomal [Fe]-hydrogenase from the anaerobic chytrid *Neocallimastix* sp L2. *Gene* **284**, 103–112 (2002).
28. van Hoek, A. H. A. M. *et al.* Voltage-dependent reversal of anodic galvanotaxis in *Nyctotherus ovalis*. *J. Eukaryotic Microbiol.* **46**, 427–433 (1999).

29. Koopman, W. J. H. *et al.* Membrane-initiated Ca²⁺ signals are reshaped during propagation to subcellular regions. *Biophys. J.* **81**, 57–65 (2001).
30. Curtis, E. A. & Landweber, L. F. Evolution of gene scrambling in ciliate micronuclear genes. *Ann. NY Acad. Sci.* **870**, 349–350 (1999).

Supplementary Information accompanies the paper on www.nature.com/nature.

Acknowledgements We thank L. Landweber, J. Wong and W.-J. Chang for advice on the cloning of complete minichromosomes and for sharing the first sequence of a PDH gene in *N. ovalis*; S. van Weelden and H. de Rooik for help in the metabolic studies; J. Brouwers for analysis of the quinones; G. Cremers, L. de Brouwer, A. Ederveen, A. Grootemaat, M. Hachmang, S. Huver, S. Jannink, N. Jansse, R. Janssen, M. Kwantes, B. Penders, G. Schilders, R. Talens, D. van Maassen, H. van Zoggel, M. Veugelink and P. Wijnhoven for help with the isolation of various *N. ovalis* sequences; and K. Sjölloma for electron microscopy. G.W.M.v.d.S., S.Y.M.-v.d.S. and G.R. were supported by the European Union 5th framework grant 'CIMES'. This work was also supported by equipment grants from ZON (Netherlands Organisation for Health Research and Development), NWO (Netherlands Organisation for Scientific Research), and the European Union 6th framework programme for research, priority 1 "Life sciences, genomics and biotechnology for health" to W.J.H.K.

Competing interests statement The authors declare that they have no competing financial interests.

Correspondence and requests for materials should be addressed to J.H.P.H. (j.hackstein@science.ru.nl). Sequences have been deposited at the EMBL database under accession numbers AF480921, AJ871267, AJ871313–AJ871361, AJ871573–AJ871576, AY608627, AY608632–AY608634, AY616150–AY616152, AY619980, AY619981, AY623917, AY623919, AY623925, AY623926, AY628683, AY628684, AY628688.

.....
Image segmentation and lightness perception

Barton L. Anderson¹ & Jonathan Winawer²

¹University of New South Wales, School of Psychology, Sydney, New South Wales 2052, Australia

²Massachusetts Institute of Technology, Brain and Cognitive Sciences, Cambridge, Massachusetts 02139, USA

The perception of surface albedo (lightness) is one of the most basic aspects of visual awareness. It is well known that the apparent lightness of a target depends on the context in which it is embedded^{1–6}, but there is extensive debate about the computations and representations underlying perceived lightness. One view asserts that the visual system explicitly separates surface reflectance from the prevailing illumination and atmospheric conditions in which it is embedded^{7–10}, generating layered image representations. Some recent theory has challenged this view and asserted that the human visual system derives surface lightness without explicitly segmenting images into multiple layers^{11,12}. Here we present new lightness illusions—the largest reported to date—that unequivocally demonstrate the effect that layered image representations can have in lightness perception. We show that the computations that underlie the decomposition of luminance into multiple layers under conditions of transparency can induce dramatic lightness illusions, causing identical texture patches to appear either black or white. These results indicate that mechanisms involved in decomposing images into layered representations can play a decisive role in the perception of surface lightness.

The amount of light projected to the eyes (luminance) is determined by a number of factors: the illumination that strikes visible surfaces, the proportion of light reflected from the surface and the amount of light absorbed, reflected or deflected by the prevailing atmospheric conditions (such as haze or other partially transparent media). Only one of these factors, the proportion of light reflected (lightness), is associated with an intrinsic property of

letters to nature

surfaces, and hence is of special interest to the visual system. To accurately recover lightness, the visual system must somehow disentangle the contributions of surface reflectance from the illumination and atmospheric conditions in which it is embedded. One theoretical view asserts that the visual system explicitly decomposes images into a set of separate maps or layers, corresponding to the separate physical contributions to retinal luminance^{9,10}. However, there is a growing body of data showing that the visual system can make systematic errors in estimating surface reflectance¹¹, the opacity of transparent surfaces or media¹³ and the amount of illumination striking a surface¹⁴. These errors have led some to question whether the visual system explicitly decomposes images

into their constituent physical sources, and to suggest that the visual system uses computational 'short cuts' to generate representations of surface lightness. Such theories have suggested that the visual system divides an image into two-dimensional regions (or 'frameworks') rather than layers. In such models, lightness is derived through processes that bias the highest luminance to appear white¹¹, and/or by using statistical estimation techniques within local image regions to compute reflectance¹²; no explicit decomposition of the image into separate layers occurs.

One of the most widely used techniques to explore context effects in lightness perception is to embed identical target patches in different surrounds. Most studies with this method have used

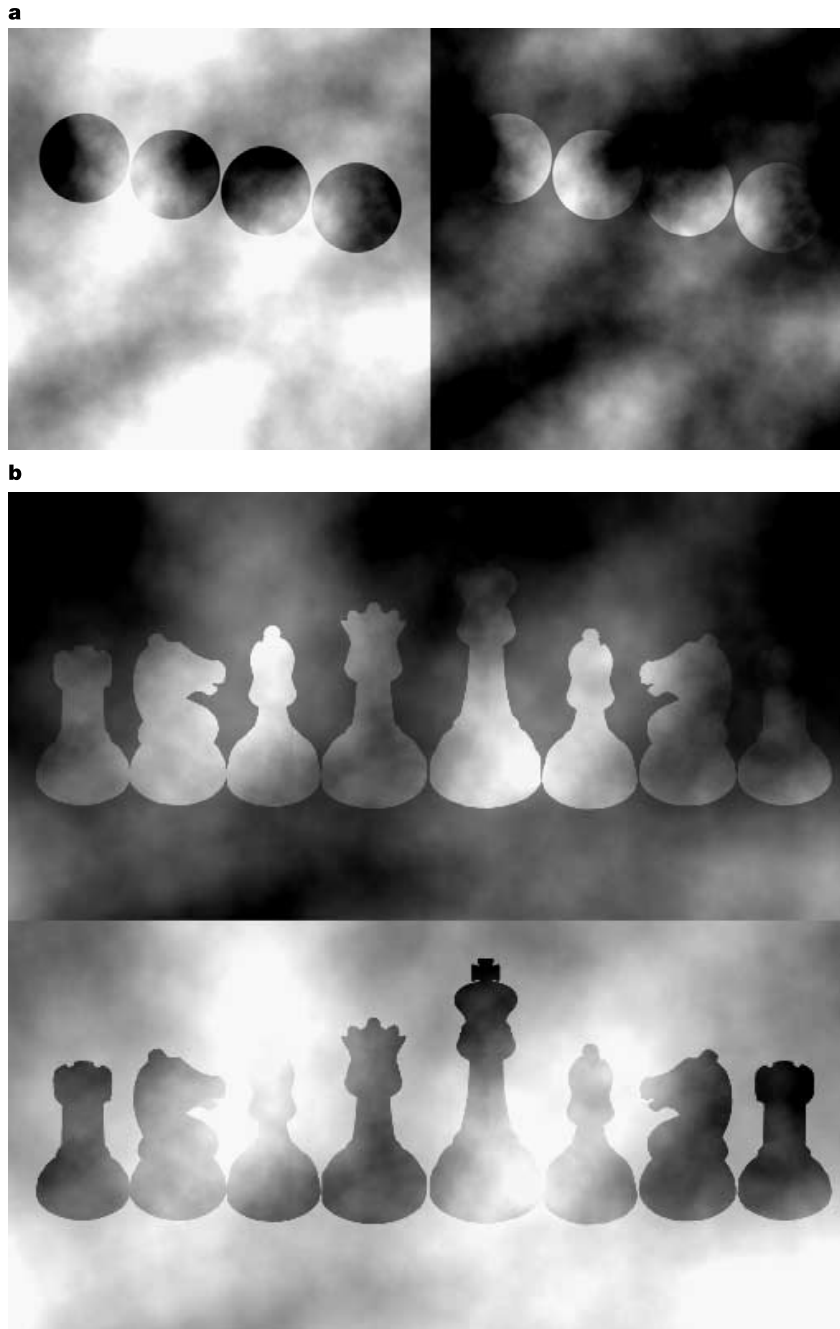


Figure 1 Static versions of the lightness illusions studied in our experiment (see also Supplementary Video 1). In **a**, the corresponding textured disks on the dark and light surrounds are physically identical, and in **b** the corresponding chess pieces on the two

surrounds are identical. In both cases, the figures on the dark surround appear as light objects visible through dark haze, whereas the figures on the light surround appear as dark objects visible through light haze.

unt textured patches containing a uniform reflectance or luminance. In such images, it is usually difficult if not impossible to determine whether a target is decomposed into multiple sources; the target region simply appears to be a particular shade of grey. To assess the role of layered image representations in perceived lightness, we devised a new set of stimuli that would make a layered decomposition perceptually apparent if it was occurring (Fig. 1). We generated textured images that contain a continuous distribution of luminance values and we also manipulated geometric and luminance relationships known to play a role in the segmentation of surfaces into multiple layers^{13,15–17}. A common ‘seed’ texture was used to create both the targets and the surrounds (see Methods). The target regions in the two images were identical; only the surrounds differed. One surround was made lighter than the seed image, and the other darker. The target regions were placed in the same relative position (compared to the seed image) on each of the two surrounds. The critical image properties manipulated using this technique were the polarity and magnitude of contrast between the textures and their surrounds. In the image with the dark surround, the polarity of the surround–target border was dark–light along its entire length of the border (respectively); in the light surround, the surround–target border was light–dark. Contrast magnitude varied continuously over both surround–target borders. As can be seen in Fig. 1 (and even more dramatically in the moving versions in Supplementary Video 1), this manipulation caused a striking difference in appearance between the central targets. For the dark surround, the target regions appeared white, visible through dark, partially transparent clouds; for the light surround, the identical targets appeared black, visible through light clouds. Note that the fluctuations in contrast magnitude along the target–surround border appear as variations in the opacity of the transparent layer; this is in keeping with recent research demonstrating that the visual system uses variations in contrast magnitude to compute the opacity of transparent layers¹³.

We performed a lightness matching experiment to determine what was responsible for the perceived lightness of the targets in these images. The targets in Fig. 1 contain luminance values that span the range from white to black. One explanation of the perceived lightness difference in these images is that the two surrounds cause the target regions to be decomposed in two very different ways. For the targets on the light surround, the darkest pixels appear to form an unobscured view of the distant surface, and lighter pixels appear to be a combination of a light transparent layer and a dark distant surface. For the targets on the dark surround, the lightest pixels appear to form an unobscured view of the distant surface, and darker pixels appear to be a combination of a dark transparent layer and a light distant surface. This decomposition is consistent with recent theory that asserts that the visual system makes use of the sign and magnitude of image contrast to determine those portions of surfaces that are in plain view and those surface regions that are obscured by transparent media¹⁵. In this account, the highest contrast regions are seen in plain view (the lightest and darkest pixels on the dark and light surrounds respectively), and lower contrast values are seen through a contrast-reducing medium (where the opacity of the transparent layer is proportional to the amount by which the highest contrast is reduced). According to this view, the entire target regions in each figure are seen to have a single lightness value as determined by the pixels in plain view. If this analysis is correct, then the perceived lightness of the light target should correspond to the perceived lightness of the brightest pixels in the target region, and the matches for the dark target should correspond to the perceived lightness of the darkest pixels in the target region.

To test this hypothesis, we varied the range of intensities in the target region (that is, its contrast), and observers adjusted the luminance of a test patch until it appeared to match the lightness of the target patches. A control experiment was performed to

determine the contribution of simple contrast enhancement mechanisms of the surrounds on uniform grey patches (see Methods and Supplementary Video 2). Results of these experiments are shown in Fig. 2. The solid lines depict the lightest and darkest pixels in the target patches (Fig. 2a). Lightness matches by the observers correspond closely to these lines, but there is also a slight overestimation of the lightness of the targets on both surrounds (the apparent saturation of the matches to the light target reflects the limited luminance range of the monitors; the luminance setting in these regions is simply the maximal available). This overestimation plays only a small part in the magnitude of the lightness transformation reported here, but it is consistent with data showing that the visual system normalizes luminance in a manner that generates a bias for observers to perceive the highest luminance as white¹¹. The contrast control experiment (Fig. 2b) showed that simple contrast enhancement processes produce a much smaller illusion (only 11% as large as the largest lightness difference with the textured targets), and therefore cannot account for the illusions in Fig. 1.

These results are consistent with the hypothesis that the transformation in lightness observed in Fig. 1 arises from segmentation processes involved in the perception of transparency. If this is correct, then such lightness transformations should be abolished if the conditions critical for inducing the perception of transparency

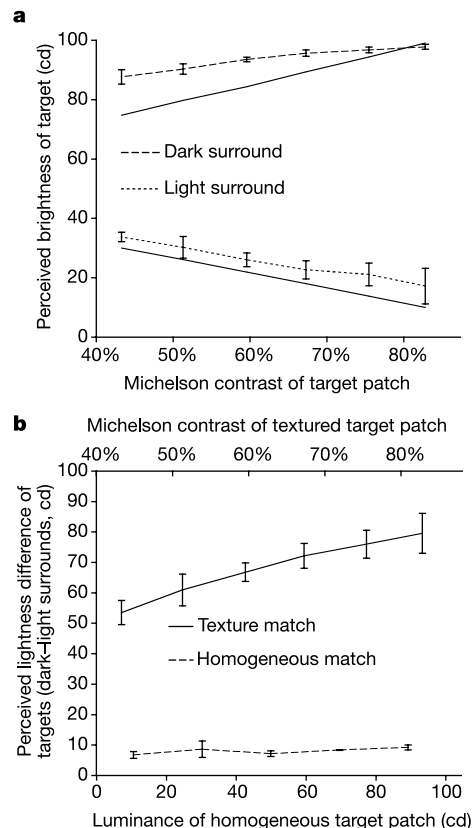


Figure 2 Lightness matching data. **a**, Data obtained using the moving version of the illusion. The light and dark surrounds were held constant, and the contrast (luminance range) of the circular target patches were varied. Solid lines depict the luminance of the lightest (upper line) and darkest (lower line) pixels in the target patch. The data are close to these lines, but there is a bias for observers to report the targets on both light and dark surrounds as lighter than these values. **b**, The data in **a** are compared with the control experiment using homogeneous targets that varied in luminance (plotted as a difference between the matches to the targets on the dark and light surrounds, respectively). The contrast effects are only 11% as large as the largest effects with the textured targets. Error bars depict the standard error of the mean for three subjects.

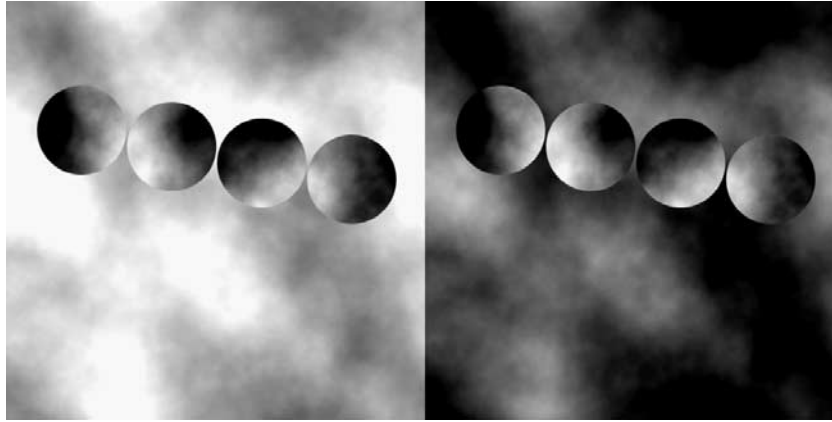


Figure 3 Transparency control experiment. The same targets and surrounds are used as in Fig. 1a, except that the surrounds have been rotated by 90° (see also Supplementary

Video 3). This rotation destroys both the geometric and luminance conditions needed to evoke a percept of transparency, and also destroys the lightness illusion.

are removed but all other aspects of the display remain unchanged. To test this hypothesis, the light and dark surrounds were simply rotated by 90°, destroying both the geometric conditions (the continuity of the textures in the targets and the surround) and the luminance relationships needed to induce the perception of transparency (the contrast polarity now reverses along the borders of both set of targets). As can be seen in Fig. 3 (and in Supplementary Video 3), this manipulation destroys the lightness difference observed in Fig. 1, demonstrating that transparency plays a critical role in the lightness transformations that occur in these displays.

The phenomena reported here provide new insights into the computations underlying lightness perception. The data are consistent with the view that lightness perception cannot be understood with low-level mechanisms such as lateral inhibition, as such mechanisms produce a much smaller illusion^{2,5,11}. Recent lightness models that omit computations that generate layered image representations also fail to account for the phenomena reported here. Such models decompose images into a set of discrete two-dimensional sub-regions, and estimate lightness within each sub-region separately using principles of anchoring¹¹ or statistical estimation¹². Note, however, that the perceived transmittance of the transparent layer appears to vary continuously over the entire image in Fig. 1. It is unclear how such models could account for these phenomena.

It should be noted that layered image representations underlying the illusions reported here are conceptually related to figure-ground reversals¹⁶. Note, however, that traditional figure-ground reversals involve shifts between image regions that occupy different regions of space, whereas the phenomena reported here involve image regions along the same visual directions, and hence involve the same set of pixels. To see this, consider the segmentation processes involved in viewing a surface through an occluding mesh or screen. In such contexts, the visual system must determine which image regions correspond to the occluding screen and which regions correspond to the underlying surface visible through the holes in the screen. This conception of transparency is readily generalized to continuous media by simply allowing the holes to become infinitesimally small. If the perceived depth order of the surfaces is reversed, then the perceived lightness of the two layers will shift as well, as can be experienced in Fig. 1.

There is a growing body of data demonstrating that a variety of factors influence perceived lightness, including surface curvature⁴, surface orientation¹⁸, depth^{2,10,11,17} and simply the number of different surfaces in a scene¹¹. Previous research has shown that transformations in perceived lightness can occur in images that

induce percepts of transparency in stereoscopic displays¹⁷. However, the causal role of such segmentation processes in lightness perception has not been previously established for monocular images. The data presented here provide unequivocal evidence that segmentation processes underlying the formation of layered image representations can play a critical and dramatic role in lightness perception. Theories of lightness perception that do not include such processes are at best incomplete. □

Methods

Textures

Textured 'seed' images were generated in Matlab as grey-scale noise with a specified power spectrum that varied as $(1/f^4)$, 512×512 pixels. The different frequency components were summed with random phases and orientations. The target and background images were spatially identical to the seed image, but differed in the range of luminance values. The target image had 99% Michelson contrast, with intensities ranging from 1 to 96 cd. For the surrounds, the luminance ranges were compressed and either shifted up or down. For the light surround (which gives rise to the percept of a dark target seen through light clouds), the range was 36 to 96 cd (45% contrast) and for the dark surround, the range was 1 to 77 cd (98% contrast). The illusions (static, Fig. 1; moving, Supplementary Video 1) were created by aligning the target texture with one of the surround textures and then showing the target through a circular aperture on either the light or dark surround. The multiple apertures in Fig. 2 represent the effect of motion. For the control demonstrations (Fig. 3), the identical targets were used but the surrounds were rotated by 90°. This caused the polarity relationships between the target patch and the surround to vary, destroying the percept of transparency and the lightness illusion.

Matching experiment

To quantify the perceived lightness in Fig. 1, subjects adjusted a test patch to match the perceived lightness of the targets. Using the stimuli described above, observers were presented with a circular target (3° in diameter) moving back and forth horizontally (one cycle every 5 s) on either a light or a dark square surround (15° per side). They adjusted the luminance of a uniform, square test patch (2°) on a black and white checkered background (3°) until the test patch appeared to be the same lightness as the moving target. Subjects had unlimited time to make the matches. Stimuli consisted of either the light or dark surrounds depicted in Fig. 1 along with one of six target stimuli similar to the target in Fig. 1, but ranging in contrast from 0.43 to 0.82. To measure the contribution of simple contrast enhancement processes to the illusion, homogenous grey disks that were identical in size to the textured targets were also presented (ranging in luminance from 10 to 89 cd), and the same matching task was used. All combinations of backgrounds (one light and one dark) and targets (six patterned and five grey) were presented five times each in random order to each subject, for a total of 55 trials.

Stimuli were generated using Vision Shell software and were presented on an Apple Macintosh G4 computer using a Lacie (electron22blue) monitor that was calibrated and linearized before testing observers. Viewing distance was 57 cm. One subject, CB, was naïve and the other two observers were the authors.

Received 13 October; accepted 13 December 2004; doi:10.1038/nature03271.

1. Koffka, K. *Principles of Gestalt Psychology* (Harcourt, Brace and World, New York, 1935).
2. Gilchrist, A. L. Perceived lightness depends on spatial arrangement. *Science* **195**, 185–187 (1977).
3. Gilchrist, A. L. When does perceived lightness depend on perceived spatial arrangement? *Percept. Psychophys.* **28**, 527–538 (1980).

4. Knill, D. C. & Kersten, D. Apparent surface curvature affects lightness perception. *Nature* **351**, 228–230 (1991).
5. Adelson, E. H. Perceptual organization and the judgment of brightness. *Science* **262**, 2042–2044 (1993).
6. Eagleman, D. M., Jacobson, J. E. & Sejnowski, T. J. Perceived luminance depends on temporal context. *Nature* **428**, 854–856 (2004).
7. Bergstrom, S. S. Common and relative components of reflected light as information about the illumination, colour, and three-dimensional form of objects. *Scand. J. Psychol.* **18**, 180–186 (1977).
8. Gilchrist, A. L. The perception of surface blacks and whites. *Sci. Am.* **240**, 112–123 (1979).
9. Barrow, H. G. & Tenenbaum, J. in *Computer Vision Systems* (eds Hanson, A. R. & Riseman, E. M.) 3–26 (Academic, New York, 1978).
10. Anderson, B. L. A theory of illusory lightness and transparency in monocular and binocular images: the role of contour junctions. *Perception* **26**, 419–453 (1997).
11. Gilchrist, A. et al. An anchoring theory of lightness perception. *Psychol. Rev.* **106**, 795–834 (1999).
12. Adelson, E. H. in *The New Cognitive Neurosciences* 2nd edn (ed. Gazzaniga, M.) 339–351 (MIT Press, Cambridge, Massachusetts, 1999).
13. Singh, M. & Anderson, B. L. Toward a perceptual theory of transparency. *Psychol. Rev.* **109**, 492–519 (2002).
14. Rutherford, M. D. & Brainard, D. H. Lightness constancy: a direct test of the illumination estimation hypothesis. *Psychol. Sci.* **13**, 142–149 (2002).
15. Anderson, B. L. The role of occlusion in the perception of depth, lightness, and opacity. *Psychol. Rev.* **110**, 762–784 (2003).
16. Anderson, B. L. The role of perceptual organization in White's illusion. *Perception* **32**, 269–284 (2003).
17. Anderson, B. L. Stereoscopic surface perception. *Neuron* **24**, 919–928 (1999).
18. Boyaci, H., Maloney, L. T. & Hersh, S. The effect of perceived surface orientation on perceived surface albedo in binocularly viewed scenes. *J. Vis.* **3**, 541–553 (2003).

Supplementary Information accompanies the paper on www.nature.com/nature.

Acknowledgements We thank N. Withoft for suggesting the chessboard variant of the illusion and C.U. Jo for inspiration and support.

Competing interests statement The authors declare that they have no competing financial interests.

Correspondence and requests for materials should be addressed to B.L.A. (bart.a@unsw.edu.au).

Cross-presentation by intercellular peptide transfer through gap junctions

Joost Neijssen^{1*}, Carla Herberths^{1*}, Jan Wouter Drijfhout², Eric Reits¹, Lennert Janssen¹ & Jacques Neeffjes¹

¹Division of Tumor Biology, The Netherlands Cancer Institute, Plesmanlaan 121, 1066 CX Amsterdam, The Netherlands

²Department of Immunohematology and Blood Transfusion Leiden, University Medical Center, Albinusdreef 2, 2333RC Leiden, The Netherlands

* These authors contributed equally to this work

Major histocompatibility complex (MHC) class I molecules present peptides that are derived from endogenous proteins¹. These antigens can also be transferred to professional antigen-presenting cells in a process called cross-presentation, which precedes initiation of a proper T-cell response^{2,3}; but exactly how they do this is unclear. We tested whether peptides can be transferred directly from the cytoplasm of one cell into the cytoplasm of its neighbour through gap junctions. Here we show that peptides with a relative molecular mass of up to ~1,800 diffuse intercellularly through gap junctions unless a three-dimensional structure is imposed. This intercellular peptide transfer causes cytotoxic T-cell recognition of adjacent, innocent bystander cells as well as activated monocytes. Gap-junction-mediated peptide transfer is restricted to a few coupling cells owing to the high cytosolic peptidase activity. We present a mechanism of antigen acquisition for cross-presentation that couples the antigen presentation system of two adjacent cells and

is lost in most tumours: gap-junction-mediated intercellular peptide coupling for presentation by bystander MHC class I molecules and transfer to professional antigen presenting cells for cross-priming.

MHC class I molecules present peptides to the immune system for surveillance by CD8⁺ cytotoxic T cells (CTL). Because intracellular antigens and antigenic peptides usually cannot traverse membranes, only endogenous peptides can be presented by MHC class I molecules¹. Antigenic peptides from infected cells are thus exclusively loaded on the cell's own MHC class I molecules and not on those of innocent bystander cells. This concept has been challenged by a process called cross-presentation^{2,3}. Cross-presentation implies the transfer of antigenic (usually intracellular) antigens from diseased cells to professional antigen-presenting cells (APC) such as dendritic cells, activated monocytes or Langerhans cells^{2–4}. The APCs subsequently present these antigenic peptides on their own MHC class I molecules, and migrate to draining lymph nodes where activation and expansion of the specific CD8⁺ T-cell population occurs. Cross-presentation requires that antigens somehow enter the MHC class I presentation pathway of an APC.

In this study, we investigated the possibility of direct gap-junction-mediated transfer of antigens between the cytoplasm of two adjacent cells. Gap junctions are assemblies of intercellular channels that form an integral part of multicellular organisms. A functional channel is formed when a hemichannel, composed of six connexin molecules, assembles with a hemichannel from an adjacent cell⁵. The resulting gap junctions electrically couple cells by direct exchange of ions and allow exchange of nutrients and second messengers. Gap junctions are thought to be non-specific channels that allow passive diffusion of molecules with a relative molecular mass of up to 1,000 (M_r 1K)⁶ and intracellular signalling controls the gating⁷. Connexin 43 (Cx43) is broadly expressed, whereas the other connexin family members are expressed in specific tissues only. Cx43 is also expressed in various haematopoietic cells like follicular dendritic cells, B cells, activated lymphocytes and monocytes⁸. Importantly, many tumour cells are uncoupled from their environment, for example after inactivation of their gap junctions by ras, src and neu oncogenes or by APC deficiency^{9,10}. Viral proteins of the herpesvirus HSV-2 (ref. 11) and the human papilloma virus HPV-16 (ref. 12) are able to close gap junctions of infected cells. In addition, gap junction intercellular communication seems to be important for the bystander effect in cancer gene therapy¹³.

To visualize peptide transfer between cells, we used A431 cells. This human squamous carcinoma cell line does not express gap junctions, as shown by biochemical and biophysical techniques¹⁴. A431 cells were stably transfected with human Cx43 (Fig. 1a), resulting in functional gap junctions. To study peptide transfer between cells, stable fluorescently labelled (FL-) peptides were synthesized. These peptides are not degraded in cells because they are composed of D-amino acids with a protective group at the amino terminus¹⁵. A 9-mer FL-peptide was introduced in A431/Cx43 and control A431 cells by micro-injection, together with dextran-TexasRed (TxR) (M_r 70K) as an injection marker. Cells were subsequently analysed by confocal laser scanning microscopy (CLSM) (Fig. 1b) and transfer was quantified in both cell lines (Fig. 1c). Whereas dextran-TxR is maintained in the micro-injected cell, the 9-mer peptide diffused into surrounding cells only when the cells expressed Cx43. Closure of gap junctions by chemical inhibitors such as 2-APB (ref. 16) prevented this intercellular peptide transfer between A431/Cx43 cells.

To test the efficiency of gap-junction-mediated peptide transfer, small groups of A431/Cx43 cells were grown on coverslips. Peptides of various lengths were micro-injected along with dextran-TxR and the rate of transfer was determined using fluorescence recovery after photobleaching (FRAP) techniques. Peptides were permitted to